

The Crystal Structures of *rac*-Bis(1,2-ethanediamine)(2-thiooxamato-*N,O*)cobalt(III) Trifluoromethanesulfonate Monohydrate at 110 and 296 K and Their Relation to the Reversible Phase Transition at 155 K

Lisbeth Grøndahl, Anders Hammershøi and Sine Larsen

Department of Chemistry, University of Copenhagen, Universitetsparken 5, DK-2100 Copenhagen, Denmark

Grøndahl, L., Hammershøi, A. and Larsen, S., 1995. The Crystal Structures of *rac*-Bis(1,2-ethanediamine)(2-thiooxamato-*N,O*)cobalt(III) Trifluoromethanesulfonate Monohydrate at 110 and 296 K and Their Relation to the Reversible Phase Transition at 155 K. – Acta Chem. Scand. 49: 792–799 © Acta Chemica Scandinavica 1995.

Crystals of *rac*-bis(1,2-ethanediamine)(2-thiooxamato-*N,O*)cobalt(III) trifluoromethanesulfonate monohydrate, *rac*-[Co(en)₂(NHC(S)COO)]CF₃SO₃·H₂O, showed a reversible phase transition at 155(2) K. Diffraction data were collected at two temperatures. At 110(5) K (LT) the space group is monoclinic $P2_1/n$, $a = 6.1509(13)$, $b = 14.872(2)$, $c = 17.421(3)$ Å, $\beta = 93.71(2)^\circ$, $V = 1590.3(8)$ Å³, $Z = 4$. Also at 295.5(5) K (RT) the space group is monoclinic $P2_1/n$, $a = 12.558(5)$, $b = 14.978(3)$, $c = 18.139(3)$ Å, $\beta = 104.44(2)^\circ$, $V = 3304(3)$ Å³, $Z = 8$. The major structural changes associated with the phase transition relate to the hydrogen bonding patterns. The geometries of the two independent complex cations in the RT structure and the cation of the LT structure are very similar. Two fluorine atoms of a trifluoromethanesulfonate anion in the RT structure display static disorder. The maximum variations between corresponding bond lengths and angles in the two structures amount to 0.06 Å and 3°, respectively.

The coordination of an amino acid to a metal centre changes the reactivity and may give rise to unusual organic chemical reactions.¹ The reaction of robust bis(1,2-ethanediamine)(glycinato)cobalt(III) ion, [Co(en)₂(NH₂CH₂COO)]²⁺, with thionyl chloride in *N,N*-dimethylformamide results in diverse modification of the chelated glycinate and, depending on conditions, various products are obtained. One such product, isolated as the chloride salt, contained one mole of sulfur per mole of cobalt. However, due to thermal instability of the complex only limited spectral data were accessible.¹ These and the analytical data left undecided the precise location and oxidation level of the sulfur atom in the complex.

The complex was crystallized as the trifluoromethanesulfonate (triflate) salt and the crystal structure analysis of this study revealed the identity of the resulting compound to be *rac*-bis(1,2-ethanediamine)(2-thiooxamato-*N,O*)cobalt(III) trifluoromethanesulfonate monohydrate, *rac*-[Co(en)₂(NHC(S)COO)]CF₃SO₃·H₂O. Furthermore, on cooling a crystal from room temperature to 110 K this compound underwent a phase transition in the solid state and the thermal behaviour was examined by differential scanning calorimetry (DSC). Structure deter-

minations at 110 K (LT) and 296 K (RT) based on data sets collected on the same crystal specimen were performed in order to clarify the overall structural changes associated with the phase transition.

Experimental

Structure determinations. Orange crystals were obtained as described¹ and their density (296 K) determined by flotation in a mixture of 1,3-diiodopropane and diethylfumarate. The same crystal specimen (dimensions 0.14 × 0.14 × 0.34 mm and tabular faces {011}, {01-1} and {101}) was used for intensity data collection at both 110(5) K (LT) and 295.5(5) K (RT) on an Enraf Nonius CAD-4 diffractometer (graphite-monochromated MoK α radiation, $\lambda = 0.71073$ Å) operating in the $\omega/2\theta$ -scan mode. Lattice parameters for the LT and the RT modifications were determined from 18 ($17.2 < \theta < 21.6^\circ$) and 22 ($15.9 < \theta < 20.8^\circ$) reflections, respectively. Scan speed intervals were 1.83–16.48° min⁻¹ (LT) and 1.27–16.48° min⁻¹ (RT) with maximum scan times of 60 s. Total intensity losses of 3.1% (LT) and 3.8% (RT), monitored for

Table 1. Crystal and experimental data for *rac*-[Co(en)₂(NHC(S)COO)]CF₃SO₃·H₂O.

Formula	CoC ₇ H ₁₈ F ₃ N ₅ O ₆ S ₂ 449.3	
Formula weight/g·mol ⁻¹		
Temperature/K	LT 105	RT 296
Space group	<i>P</i> 2 ₁ / <i>n</i>	<i>P</i> 2 ₁ / <i>n</i>
<i>a</i> /Å	6.1509(13)	12.558(5)
<i>b</i> /Å	14.872(2)	14.978(3)
<i>c</i> /Å	17.421(3)	18.139(3)
β/°	93.71(2)	104.44(2)
<i>V</i> /Å ³	1590.3(8)	3304(3)
<i>Z</i>	4	8
<i>d</i> _{calc} /g cm ⁻³	1.868	1.806
<i>d</i> _{obs} /g cm ⁻³	—	1.775
μ/cm ⁻¹ (λ=0.710 73 Å)	13.957	13.439
Scan width/°	(1.2+0.35 tan θ)	0.8+0.35 tan θ
Standard reflections	(020),(105),(200)	(01-2),(020),(200)
θ range/°	<i>hk±l</i> : 1-31	<i>hk±l</i> : 1-30 <i>h-k±l</i> : 1-25 ^a
Range of indices	0 < <i>h</i> < 8 0 < <i>k</i> < 21 -25 < <i>l</i> < 25	0 < <i>h</i> < 17 -17 < <i>k</i> < 21 -25 < <i>l</i> < 24
No. of reflections:		
measured	5712	13605
independent	5046	9617
<i>R</i> _{int}	0.0022	0.029
observed	3464	4404
<i>I</i> /σ(<i>I</i>) criterion	2	1
No. of variables	274	535
<i>R</i> ^b	0.038	0.043
<i>R</i> _w	0.043	0.043
Max. shift/error [(Δ/σ) _{max}]	0.05	0.28
Max./Min. Δρ/e Å ⁻³	0.6/-0.7	0.5/-0.4
<i>S</i>	1.23	1.06

^a Range only partially covered. ^b $R = \frac{\sum_h | |F_o(h)| - |F_c(h)| |}{\sum_h |F_o(h)|}$

every 10000 s for three standard reflections (Table 1) were considered insignificant and no corrections were applied. Data sets were corrected for Lorentz, polarization and absorption effects. Transmission factors, within the ranges 0.799–0.842 (LT) and 0.816–0.850 (RT), were calculated by the Gaussian numerical integration procedure. Crystal data and further experimental details relating to data collections and structure refinements are given in Table 1. Computations were carried out with the SDP package² employing atomic scattering factors, including contributions from anomalous scattering,³ as contained in the program. All non-hydrogen atoms were located by Patterson and Fourier methods and refined by least squares, minimizing $\sum w(|F_o| - |F_c|)^2$ with weights $w = [\sigma^2(F) + 0.00041 |F|^2]^{-1}$ and $\sigma^2(F)$ calculated from counting statistics. After the introduction of anisotropic displacement parameters, the hydrogen atom positions were clearly located in the LT structure and their positional parameters subsequently refined with the isotropic thermal parameter fixed at $B = 2.0 \text{ \AA}^2$. For the RT structure not all hydrogen atoms could be localized in a difference electron density map and hydrogen atoms of the complex cation were refined after being introduced in idealized positions and were given a fixed isotropic temperature factor 1.3 times that of the nearest atom.

Table 2. Fractional coordinates and isotropic thermal parameters for non-hydrogen atoms of the LT structure.

Atom	<i>x</i>	<i>y</i>	<i>z</i>	<i>B</i> _{iso}
Co	0.24735(5)	-0.12882(5)	0.14364(2)	0.966(5)
S1	0.4183(1)	0.15172(5)	0.09522(4)	1.70(1)
O1	0.5289(3)	-0.1080(1)	0.1072(1)	1.16(3)
O2	0.7490(3)	0.0003(1)	0.0709(1)	1.51(3)
N1	0.2263(4)	-0.0018(2)	0.1376(1)	1.47(4)
N2	-0.0328(3)	-0.1440(2)	0.1889(1)	1.40(4)
N3	0.3708(3)	-0.1219(2)	0.2499(1)	1.26(4)
N4	0.3004(3)	-0.2585(2)	0.1376(1)	1.17(4)
N5	0.1143(4)	-0.1394(2)	0.0392(1)	1.48(4)
C1	0.5743(4)	-0.0252(2)	0.0942(2)	1.12(4)
C2	0.3920(4)	0.0408(2)	0.1110(2)	1.28(4)
C4	0.0060(4)	-0.1688(2)	0.2712(2)	1.51(5)
C5	0.1919(4)	-0.1108(2)	0.3031(2)	1.60(5)
C6	0.2779(5)	-0.2850(2)	0.0554(2)	1.61(5)
C7	0.0830(5)	-0.2354(2)	0.0193(2)	1.79(5)
S2	0.6646(1)	0.08262(4)	0.32031(4)	1.15(1)
F1	0.9666(3)	0.0211(1)	0.4191(1)	2.14(3)
F2	0.6758(3)	0.0653(1)	0.4706(1)	2.25(3)
F3	0.6759(3)	-0.0603(1)	0.4080(1)	2.46(4)
O3	0.7468(3)	0.1728(1)	0.3333(1)	1.48(3)
O4	0.7666(3)	0.0314(1)	0.2623(1)	1.68(4)
O5	0.4304(3)	0.0761(1)	0.3171(1)	1.77(4)
C3	0.7502(5)	0.0241(2)	0.4094(2)	1.64(5)
O6	0.5129(4)	-0.2894(2)	0.3161(1)	2.30(4)

Atomic fractional coordinates for all non-hydrogen atoms appear in Tables 2 and 3. The RT modification contains two formula units per asymmetric unit and atoms are denoted A1_{nm} and A2_{nm} corresponding to A_{nm} in the LT modification. Tables of anisotropic displacement parameters, positional parameters for hydrogen atoms and a listing of observed and calculated structure amplitudes are available from the authors on request.

Phase transition. The phase transition temperature was estimated by recording the intensities at nine different temperatures (between 110 and 293 K) of a low-order reflection which was present at the higher temperature

but absent at the lower temperature; the thermoelement was not calibrated in this range and significant hysteresis was observed.

DSC traces were recorded on a Polymer Laboratories differential scanning calorimeter (PL DSC), calibrated with Hg and Ga. A heating rate of 10° min⁻¹ was applied for the temperature range 130–310 K for a sample of 15.411 mg.

Results and discussion

Crystal structure determinations were performed at 110 K (LT) and 296 K (RT). The LT structure contains

Table 3. Fractional coordinates and isotropic thermal parameters for non-hydrogen atoms of the RT structure.

Atom	x	y	z	B _{iso}
Co1	0.45920(4)	-0.12000(4)	0.15465(3)	2.13(1)
S11	0.36302(9)	0.16103(8)	0.11140(8)	3.76(3)
O11	0.3062(2)	-0.0948(2)	0.1222(2)	2.46(6)
O12	0.1856(2)	0.0156(2)	0.0940(2)	3.11(7)
N11	0.4712(3)	0.0065(2)	0.1517(2)	3.06(8)
N12	0.6164(2)	-0.1403(2)	0.1979(2)	2.83(7)
N13	0.4492(3)	-0.1167(2)	0.2605(2)	2.77(7)
N14	0.4247(2)	-0.2479(2)	0.1439(2)	2.51(7)
N15	0.4737(3)	-0.1279(2)	0.0502(2)	2.98(7)
C11	0.2815(3)	-0.0117(3)	0.1131(2)	2.32(8)
C12	0.3802(3)	0.0513(3)	0.1275(2)	2.50(8)
C14	0.6363(3)	-0.1645(3)	0.2790(3)	3.2(1)
C15	0.5610(3)	-0.1062(3)	0.3114(3)	3.6(1)
C16	0.3954(4)	-0.2707(3)	0.0621(3)	3.4(1)
C17	0.4731(4)	-0.2218(3)	0.0263(3)	3.7(1)
Co2	-0.06743(4)	-0.13521(3)	0.11862(3)	2.06(1)
S21	-0.14651(9)	0.14819(7)	0.07224(7)	3.44(3)
O21	-0.2192(2)	-0.1041(2)	0.0975(2)	2.29(6)
O22	-0.3339(2)	0.0097(2)	0.0651(2)	3.28(7)
N21	-0.0503(2)	-0.0117(2)	0.1028(2)	2.61(7)
N22	-0.1064(2)	-0.2611(2)	0.1253(2)	2.42(7)
N23	-0.0521(3)	-0.1146(2)	0.2267(2)	2.77(7)
N24	0.892(2)	-0.1586(2)	0.1461(2)	2.94(8)
N25	-0.0781(3)	-0.1611(2)	0.0115(2)	3.02(8)
C21	-0.2404(3)	-0.0209(3)	0.0819(2)	2.45(8)
C22	-0.1387(3)	0.0369(3)	0.0869(2)	2.41(8)
C24	0.1282(3)	-0.1651(4)	0.2298(3)	4.2(1)
C25	0.0649(4)	-0.1011(4)	0.2657(3)	4.3(1)
C26	-0.1581(4)	-0.2934(3)	0.0473(3)	3.4(1)
C27	-0.0924(4)	-0.2578(3)	-0.0036(3)	3.6(1)
S12	0.33704(8)	0.41665(7)	0.80762(6)	2.86(2)
F11	0.2596(3)	0.4915(2)	0.9128(2)	6.17(8)
F12	0.3979(3)	0.5576(2)	0.8912(2)	6.73(9)
F13	0.4181(3)	0.4344(2)	0.9536(2)	7.1(1)
O13	0.3039(2)	0.3294(2)	0.8257(2)	4.02(7)
O14	0.4442(3)	0.4178(2)	0.7932(2)	4.86(8)
O15	0.2572(3)	0.4676(2)	0.7555(2)	5.02(9)
C13	0.3562(4)	0.4787(3)	0.8963(3)	4.2(1)
S22	0.33700(8)	0.08612(7)	0.33894(6)	2.81(2)
F21	0.2166(2)	0.0150(2)	0.4212(2)	6.43(8)
F22	0.3612(4)	-0.0569(3)	0.4191(3)	11.0(1)
F23	0.3719(3)	0.0608(4)	0.4836(2)	10.0(1)
O23	0.4527(3)	0.0875(2)	0.3465(2)	4.95(9)
O24	0.2918(3)	0.1709(2)	0.3489(2)	5.16(9)
O25	0.2774(3)	0.0337(3)	0.2769(2)	5.31(9)
C23	0.3217(5)	0.0238(4)	0.4207(3)	4.9(1)
O16	0.3994(3)	-0.2978(2)	0.3093(2)	4.65(8)
O26	0.6084(3)	0.2286(3)	0.1920(2)	5.31(9)

three separate species: the complex cation, the triflate anion and a water molecule, whereas the RT structure comprises two crystallographically independent entities of each species.

The complex cations. Drawings of the *rac*-[Co(en)₂(NHC(S)COO)]⁺ cation in the LT modification and the two independent cations in the RT modification are shown in Fig. 1. Interatomic distances and angles within each of the three crystallographically different cations are listed in Table 4; atom labelling allows direct comparisons of corresponding distances and angles.

All three cations display almost identical octahedral geometries; the largest deviations are observed for the 'Co2' (RT) cation for which the Co2–N22 bond length is 1.937(3) Å and the N22–C24–C25 bond angle is 109.3(4)° compared with Co–N2 [1.954(2) Å] and N2–C4–C5 [106.6(2)°], and Co1–N12 [1.958(3) Å] and N12–C14–C15 [106.3(4)°] for the 'Co' (LT) and 'Co1' (RT) cations, respectively.

For complex ions with Δ absolute configuration the two five-membered chelate rings of the ' Δ -Co(en)₂' moieties adopt the δ,λ (N2N3,N4N5) conformations in all three cations. The magnitudes of individual bond lengths and angles within these segments agree with those of similar systems.^{4,5}

The *O,N*-bound ligand of doubly deprotonated 2-thiooxamic acid, here referred to as 'thiooxamate', is essentially planar with all torsional angles less than 5°. The C2–S1 and N1–C2 distances in the three cations are all similar falling within the ranges 1.67–1.69 and 1.30–1.31 Å, respectively. In general, *N*-coordination of a carboxamide to a metal centre with proton loss affects the structure of the amide segment. For peptides, such coordination typically leads to an increase of the peptide C–O bond distance (to ca. 1.27 Å from ca. 1.24 Å) and a decrease of the carboxamidate C–N bond distance (to ca. 1.30 Å from ca. 1.33 Å).⁶ Such structural changes are ascribed to a relative shift of electron density from the N atom towards the O atom as a consequence of the poorer polarising ability of the metal centre compared with the proton.⁷ This would lead to increased double-bond character of the C–N bond. The thiocarboxamidate C–N bond distances (1.30–1.31 Å) of this study are close to the quoted average value of 1.30 Å for *N*-coordinated carboxamidates.⁶ However, no effect of coordination on the C–S bond distance is discernable. Thus, the C2–S1 bond distances (1.67–1.69 Å) are within the range of 1.64–1.69 Å observed for free, i.e. non-coordinated, thiocarboxamides^{8–15} and data for free thiooxamate are lacking. However, the average S1–C2–N1 angle of 128(1)° is larger (by ca. 5°) and the average N1–C2–C1 angle of 110.4(3)° correspondingly smaller than the equivalent angles in free thiocarboxamides.^{8–15} This may reflect some adjustment to the bonding requirements of the metal centre.

The average Co–N1 distance of 1.897(6) Å is significantly shorter than any of the Co–N (primary amine)

distances in the structure but agrees with Co–N (amidate) distances found in other structures of coordinated carboxamidates.^{16,17}

The triflate anions. As expected, the thermal ellipsoids of the RT structure are generally much larger than those of the LT study. Consequently, the C–F and S–O distances of the RT modification are significantly shortened compared with the anion of the LT modification. Both temperatures are significantly above the Debye temperature of the compound. Therefore, the temperature factors are expected to be proportional to the absolute temperature.¹⁸ Comparisons of relevant temperature factors (Tables 2 and 3) reveal this to be borne out for all atoms except for two fluorine atoms of the 'S22' (RT) anion. This is consistent with static disorder of these two fluorine atoms, also implied by the shortening of the C–F bonds. The variations between corresponding bond lengths of all three triflate ions were within 0.06 Å.

Crystal packing. Hydrogen bonding dominates the crystal packing at both temperatures, but the bonding pattern of individual cations differ markedly (Table 5). Potential hydrogen-bond donors are the four coordinated amine groups, the amido group of the complex cation and the water molecule. The 'Co' (LT) cation hydrogen bonds with seven of the eight amine hydrogen atoms to three different anions, two other cations and a water molecule. The 'Co1' (RT) cation employs all amine protons in hydrogen bonding to four different anions, two other cations and a water molecule. Thus, apart from the extra anion interaction for the 'Co1' (RT) cation the two cations display similar patterns. By contrast, the different hydrogen bonding pattern of the 'Co2' (RT) cation includes the amido group. This cation is hydrogen-bonded to two other cations, two different anions and a water molecule. The differences in crystal packing are evident from the stereoscopic diagrams in Figs. 2 and 3.

Only one of the water protons of the LT structure engages in hydrogen bonding and donates to S1 of a complex ion. However, this water molecule links two complex ions (related by the 2₁ axis) by also accepting an amine proton from another cation. The two crystallographically different water molecules in the RT structure each accept an amine proton in analogy to the LT structure. However, since the hydrogen atoms of these water molecules were not located with certainty in the electron density map the question arises whether the O6...S1 hydrogen bond of the LT structure is retained in the RT structure. The 'O26' (RT) water molecule, which accepts a proton from N23 of the 'Co2' (RT) cation, gives an O26...S11 distance [3.226(4) Å] close to the O6...S1 distance [3.273(2) Å] of the LT structure. In addition, one of the peaks above noise level in the final difference electron density map was found in a position that corresponds to the expected position of the proton of the O26...S11 hydrogen bond. For the other water molecule, 'O16' (RT), the shortest distance to S21 [3.403(4) Å] is significantly longer than the

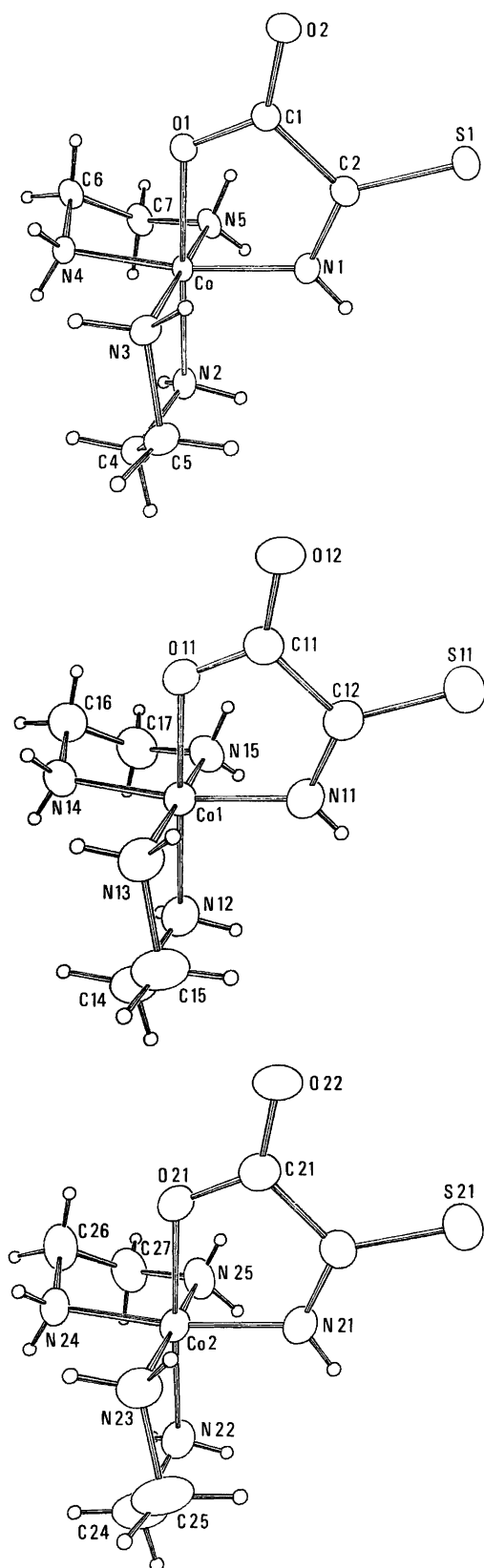


Fig. 1. ORTEP drawings of the three crystallographically different cations centred on 'Co' (LT), 'Co1' (RT) and 'Co2' (RT). The drawing of the 'Co' (LT) cation corresponds to the mirror image of the cation defined by the coordinates in Table 2.

Table 4. Bond lengths (in Å), bond angles (in °), and torsion angles (in °) for the $[\text{Co}(\text{en})_2(\text{OOCSSNH})]^+$ cations centered on 'Co'(LT), 'Co1'(RT) and 'Co2'(RT), respectively, of the two crystal structures.

	'Co'(LT)	'Co1'(RT)	'Co2'(RT)
Co—O1	1.908(2)	1.902(2)	1.905(3)
Co—N1	1.896(2)	1.903(4)	1.892(4)
Co—N2	1.954(2)	1.958(3)	1.937(3)
Co—N3	1.958(2)	1.956(4)	1.946(4)
Co—N4	1.960(2)	1.964(3)	1.959(4)
Co—N5	1.953(2)	1.951(4)	1.952(4)
O1—C1	1.286(3)	1.282(5)	1.292(5)
O2—C1	1.233(3)	1.237(4)	1.226(4)
N1—C2	1.310(4)	1.304(5)	1.298(5)
N2—C4	1.485(4)	1.475(6)	1.478(6)
N3—C5	1.493(4)	1.485(5)	1.477(6)
N4—C6	1.483(4)	1.477(6)	1.484(5)
N5—C7	1.479(4)	1.472(6)	1.477(6)
C2—S1	1.682(3)	1.674(4)	1.685(4)
C1—C2	1.533(3)	1.528(5)	1.528(5)
C4—C5	1.510(4)	1.510(7)	1.495(8)
C6—C7	1.509(4)	1.492(7)	1.483(7)
O1—Co—N1	83.10(9)	82.8(1)	82.9(1)
O1—Co—N2	175.03(9)	174.2(2)	175.2(2)
O1—Co—N3	90.07(8)	89.5(1)	90.4(1)
O1—Co—N4	89.10(8)	89.0(1)	89.7(1)
O1—Co—N5	92.15(9)	92.5(1)	91.8(1)
N1—Co—N2	94.5(1)	95.0(2)	94.0(2)
N1—Co—N3	91.2(1)	91.6(2)	90.7(2)
N1—Co—N4	171.3(1)	170.5(2)	171.8(2)
N1—Co—N5	90.3(1)	90.3(2)	91.4(2)
N2—Co—N3	85.59(9)	85.2(2)	86.0(2)
N2—Co—N4	93.54(9)	93.7(2)	93.6(2)
N2—Co—N5	92.24(9)	92.9(2)	91.9(2)
N3—Co—N4	92.70(9)	93.2(2)	93.1(2)
N3—Co—N5	177.45(9)	177.4(2)	177.1(2)
N4—Co—N5	86.09(9)	85.2(2)	85.1(2)
Co—O1—C1	115.2(2)	115.2(2)	114.9(2)
Co—N1—C2	116.7(2)	116.9(3)	117.4(3)
Co—N2—C4	109.1(2)	109.9(3)	109.4(3)
Co—N3—C5	109.7(2)	109.4(3)	110.0(3)
Co—N4—C6	107.9(2)	108.6(3)	108.1(3)
Co—N5—C7	109.7(2)	110.5(3)	110.8(3)
O1—C1—O2	123.8(2)	123.0(4)	123.2(4)
O1—C1—C2	114.2(2)	114.7(3)	114.3(3)
O2—C1—C2	122.0(2)	122.3(4)	122.5(4)
S1—C2—N1	128.1(2)	128.9(3)	127.2(3)
S1—C2—C1	121.2(2)	120.9(3)	122.4(3)
N1—C2—C1	110.7(2)	110.2(4)	110.4(4)
N2—C4—C5	106.6(2)	106.3(4)	109.3(4)
N3—C5—C4	106.2(2)	106.4(4)	106.1(4)
N4—C6—C7	107.1(2)	107.3(4)	107.3(4)
N5—C7—C6	106.6(2)	107.2(4)	107.3(3)
N1—Co—O1—C1	-1.4(2)	0.4(3)	1.2(3)
O1—Co—N1—C2	2.5(2)	-3.3(3)	0.1(3)
Co—O1—C1—C2	0.2(3)	2.1(4)	-2.1(4)
Co—N1—C2—C1	-2.8(3)	4.9(5)	-1.2(4)
O1—C1—C2—N1	1.7(3)	-4.5(5)	2.1(5)
O2—C1—C2—S1	2.2(4)	-4.7(6)	2.8(6)
N3—Co—N2—C4	-16.5(2)	14.2(3)	10.4(3)
N2—Co—N3—C5	-12.6(2)	15.0(3)	16.3(3)
Co—N2—C4—C5	41.6(2)	-39.6(4)	-35.0(4)
Co—N3—C5—C4	38.2(2)	-40.2(4)	-38.6(4)
N2—C4—C5—N3	-51.5(3)	51.5(4)	47.7(5)
N5—Co—N4—C6	17.0(2)	-17.2(3)	-19.5(3)
N4—Co—N5—C7	11.7(2)	-10.7(3)	-7.9(3)
Co—N4—C6—C7	-41.6(2)	41.1(4)	43.0(4)
Co—N5—C7—C6	-37.2(3)	35.8(4)	33.6(4)
N4—C6—C7—N5	51.5(3)	-50.0(4)	-49.7(5)

Table 5. Hydrogen-bonding interactions²³ in LT and RT structures of *rac*-[(en)₂Co(OOCCSNH)]O₃SCF₃·H₂O.

LT structure:	O—H···S	H···S	O—H···S
	N—H···O	H···O	N—H···O
'Co' cation	/Å	/Å	/°
N2—H21···O3 ^a	3.039(3)	2.29(4)	147(3)
N2—H22···O4 ^b	3.189(3)	2.41(3)	141(3)
N3—H31···O6	2.860(3)	1.95(3)	161(3)
N4—H41···O5 ^a	2.972(3)	2.19(3)	150(3)
N4—H42···O3 ^c	2.979(3)	2.25(4)	161(3)
N5—H51···O2 ^b	3.136(3)	2.35(3)	150(3)
N5—H52···O2 ^d	2.978(3)	2.21(3)	146(3)
O6—H61···S1 ^a	3.273(2)	2.45(4)	168(3)
RT structure:			
'Co1' cation			
N12—H121···O15 ^e	3.160(5)	2.37(5)	143(4)
N12—H122···O13 ^f	3.069(5)	2.38(5)	142(5)
N13—H131···O16	2.968(5)	2.14(5)	161(4)
N13—H132···O25	3.184(6)	2.33(5)	170(4)
N14—H141···O24 ^g	3.011(5)	2.27(4)	146(4)
N14—H142···O14 ^f	3.090(5)	2.33(5)	159(4)
N15—H151···O22 ^g	3.136(5)	2.43(5)	156(5)
N15—H152···O22 ^h	2.960(5)	2.15(5)	156(4)
O26···S11 ⁱ	3.226(4)		
'Co2' cation			
N21—H211···O12	3.034(4)	2.27(4)	152(4)
N22—H221···O12	3.120(5)	2.32(5)	171(4)
N22—H222···O24 ^g	2.949(5)	2.20(5)	141(4)
N23—H231···O26 ^g	2.952(6)	2.04(5)	161(4)
N23—H232···O15 ^f	3.388(6)	2.60(5)	163(4) ^k
N23—H232···O14 ^f	3.190(5)	2.55(5)	135(4) ^k
N24—H241···O13 ^f	3.015(5)	2.29(5)	145(4)
N24—H242···O23 ^g	2.939(5)	2.16(5)	157(5)
N25—H252···O12 ^h	2.991(5)	2.33(5)	150(5)
O16···S21 ⁱ	3.403(4)		

^a (1/2-x, y-1/2, 1/2-z). ^b (x-1, y, z). ^c (1/2-x, y-1/2, 1/2-z). ^d (1-x, -y, -z). ^e (x-1/2, -1/2-y, z-1/2). ^f (1-x, -y, 1-z). ^g (1+x, y, z). ^h (x, -y, -z). ⁱ (x-1/2, -1/2-y, z-1/2). ^j (-x, -y, 1-z). ^k The bond length criteria for hydrogen bonding: X—H···Y max. 3.4 Å, H···Y max. 2.4 Å,²³ are not fulfilled. ^l Suggested hydrogen bond interaction.

previous O···S distances and, furthermore, cannot be classified as a hydrogen bond, since the distance is close to the sum of the van der Waals radii of the two atoms. Thus, in the RT structure at least one O···S hydrogen-bond interaction is found which is analogous to the O6—H61···S1 hydrogen bond of the LT structure.

The crystal structures and the phase transition. The LT (110 K) and the RT (296 K) structures both belong to the space group $P2_1/n$, but display unit-cell dimensions which qualitatively differ by what essentially amounts to a doubling of the *a*-axis and some opening (by ca. 10°) of the β angle for the RT structure compared with the LT modification. The structural changes associated with the phase transition correspond almost exclusively to changes in the *ac*-plane as evidenced by the unit cell parameters and the atomic coordinates. The two cations of the RT structure are almost related by pseudo-translational symmetry, but a direct comparison of coordinates is not meaningful since the β angles for the two modifications differ. Figure 4 represents a superimposed projection onto the *ac*-plane of the unit cells of the RT and the LT structures. In order to allow easy comparison of relative positions only the positions of the cation cobalt and anion sulfur atoms are included in the diagram. Evidently, the relative positions of the cations and anions are only slightly affected by the phase transition.

In conclusion, the major structural differences between the two phases relate to the hydrogen-bonding pattern. Relative positions of individual molecular entities and their geometries are only marginally affected; the largest difference, associated with static disorder, is seen for one of the triflate ions.

The intensities of a single reflection, monitored at different temperatures implied a discontinuity near 130 K. The DSC trace for *rac*-[Co(en)₂(NHC(S)COO)]-CF₃SO₃·H₂O (temp. range 130–310 K; heating rate: 10°C min⁻¹) revealed an endothermic transition ($\Delta H \approx 3.5$ kJ mol⁻¹) at 155 ± 2 K (on set temperature) as the only feature. This is ascribed to the phase transition

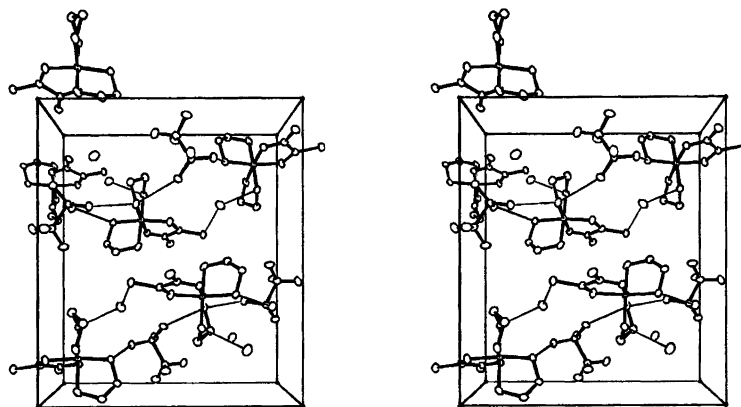


Fig. 2. Stereo pair viewed along the *a*-axis illustrating the crystal packing of the structure at 110 K (LT). Hydrogen bonds are indicated as thin lines.

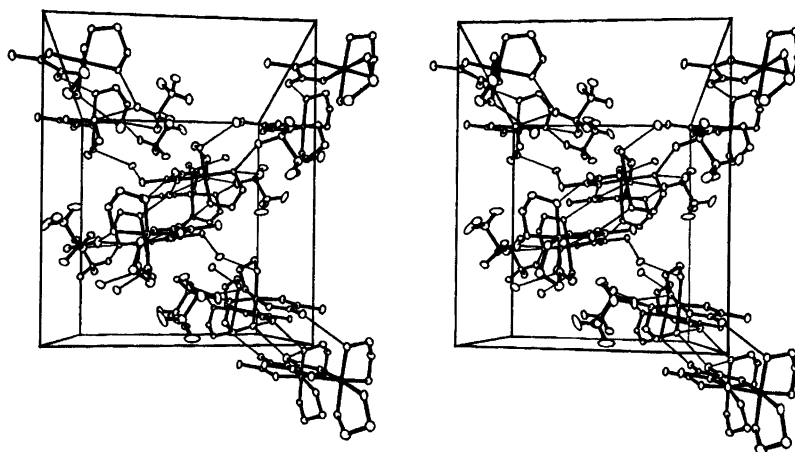


Fig. 3. Stereo pair viewed along the *a*-axis illustrating the crystal packing of the structure at 296 K (RT). Hydrogen bonds are indicated as thin lines.

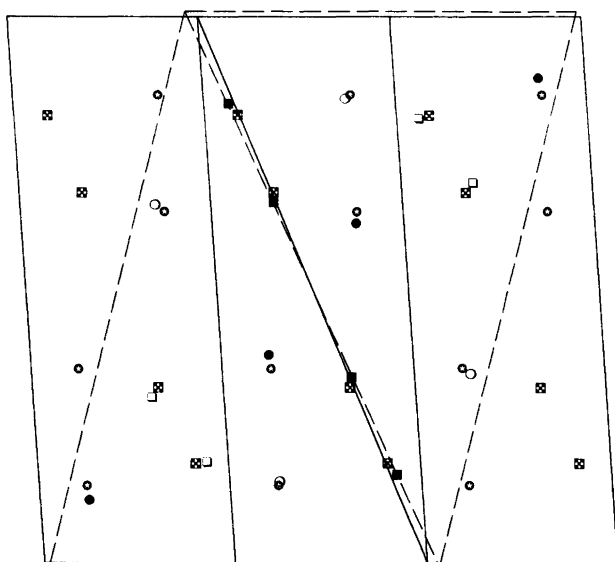


Fig. 4. Unit-cell projections onto the *ac*-planes of the RT and the LT structures (*a*-axes horizontal). One unit cell projection for the RT modification is represented by broken lines and three unit cells of the LT modification are represented by full-drawn lines. Cobalt atom positions are indicated by \odot [*'Co'* (LT)], \circ [*'Co1'* (RT)] and \bullet [*'Co2'* (RT)], and sulfur atoms of the triflate ions are indicated by \boxtimes [*'S2'* (LT)], \square [*'S12'* (RT)] and \square [*'S22'* (RT)]. With the *a*-axes parallel the two projections are qualitatively superpositioned so that all distances between corresponding atoms of the two structures are minimized, overall. The *ac*-plane diagonals (each of which indicates the translational symmetry direction of the glide planes) almost coincide.

implied by the structural results and is in accord with the result of the intensity measurement. The positive ΔH value implies a first-order phase transition.

Generally, salts of coordination complexes seldom undergo solid-state phase transitions in the range 110–298 K. Why does it occur in the present case? Related coordination compounds which normally do not exhibit

such phase transitions are typically characterized by comparable numbers of hydrogen donor atoms and likely acceptor atoms.^{4,19,20} In this respect, the empirical hydrogen bond rules formulated by Donohue²¹ for organic structures, and later elaborated by Etter,²² are obeyed. The present compound, however, provides 11 hydrogen atoms for hydrogen bonding but only 6 potential acceptor atoms. Thus, the different hydrogen bonding patterns of the RT and LT structures may reflect an inability of the present compound in attaining an optimal arrangement allowing all potential hydrogen-bond donors to be engaged in hydrogen bonding. The doubling of the asymmetric unit volume and the increased triflate ion disorder are consistent with the higher entropy of the RT modification implied by the endothermic nature of the phase transition.

Acknowledgements. Support from the Danish Natural Science Research Council and The Lundbeck Foundation (DSC equipment) is gratefully acknowledged. The authors also thank Mr. Flemming Hansen for assistance with the experimental crystallography and Ms. Katalin Marthi for DSC measurements.

References

1. Grøndahl, L., Hammershøi, A., Hartshorn, R. M. and Sargeson, A. M. *Acta Chem. Scand.* 49 (1995) 781.
2. *Enraf-Nonius Structure Determination Package, VAX version* Enraf-Nonius, Delft, The Netherlands 1985.
3. *International Tables for X-Ray Crystallography*, Kynoch Press, Birmingham 1974, Vol. 4.
4. Gajhede, M. and Larsen, S. *Acta Crystallogr., Sect. B* 42 (1986) 172.
5. Curtis, N. J., Hammershøi, A., Nicolas, L. M., Sargeson, A. M. and Watson, K. J. *Acta Chem. Scand., Ser. A* 41 (1987) 36.
6. Sigel, H. and Martin, R. B. *Chem. Rev.* 82 (1982) 385.
7. Dixon, N. E. and Sargeson, A. M. In: Spiro, T. G., Ed., *Zinc Enzymes*, Wiley, New York 1983, Chap. 7.

8. Roques, P. R., Lamazouère, A. M., Sotiropoulos, J., Declercq, J. P. and Germain, G. *Acta Crystallogr., Sect. B* 36 (1980) 1569.
9. Shoja, M. and White, J. G. *Acta Crystallogr., Sect. B* 35 (1979) 206.
10. Brunskill, J. S. A., De, A., Ewing, D. F. and Welch, A. J. *Acta Crystallogr., Sect. C* 40 (1984) 493.
11. Shoja, M. and Kaloustain, M. K., *Acta Crystallogr., Sect. C* 39 (1983) 1057.
12. Shoja, M. and Kaloustain, M. K. *Z. Krist.* 164 (1983) 13.
13. Lindley, P. F., Baydar, A. E. and Boyd, B. V. *Acta Crystallogr., Sect. C* 41 (1985) 1277.
14. Form, G. R., Raper, E. S. and Downie, T. C. *Acta Crystallogr., Sect. B* 29 (1973) 776.
15. Adiwidjaja, G., Günter, H. and Woss, J. *Liebigs Ann. Chem.* (1983) 1116.
16. Schneider, M. L., Ferguson, G. and Balahura, R. J. *Can. J. Chem.* 51 (1973) 2180.
17. Barnet, M. T. and Freeman, H. C. *J. Chem. Soc., Chem. Commun.* (1970) 367.
18. Willis, B. M. T. and Pryor, A. W. *Thermal Vibrations in Crystallography*, Cambridge University Press, Cambridge 1975.
19. Larsen, E., Larsen, S., Poulsen, G. B., Springborg, J. and Wany, D. N. *Acta Chem. Scand.* 48 (1994) 107.
20. Jacobsen, C. J. H., Hyldtoft, J., Larsen, S. and Pedersen, E. *Inorg. Chem.* 33 (1994) 840.
21. Donohue, J. J. *J. Phys. Chem.* 56 (1952) 502.
22. Etter, M. C. *J. Phys. Chem.* 95 (1991) 4601.
23. Olovsson, I. and Jonsson, P. G. In: Schuster, P., Zundel, G. and Sandorfy, C., Ed., *The Hydrogen Bond/II* North-Holland, Amsterdam 1976, Chap. 8.

Received October 22, 1994.